The Journal of Neuroscience, March 1, 2001, 21(5):1421–1433

synaptotagmin Mutants Reveal Essential Functions for the C2B Domain in Ca^{2+}-Triggered Fusion and Recycling of Synaptic Vesicles *In Vivo*

J. Troy Littleton,[4] Jihong Bai,[1] Bimal Vyas,[1] Radhika Desai,[1] Andrew E. Baltus,[4] Martin B. Garment,[2] Stanley D. Carlson,[2] Barry Ganetzky,[3] and Edwin R. Chapman[1]

Departments of [1]Physiology and [2]Entomology, and [3]Laboratory of Genetics, University of Wisconsin, Madison, Wisconsin 53706, and [4]Center for Learning and Memory and Department of Biology, Massachusetts Institute of Technology, Cambridge, Massachusetts 02139

Synaptotagmin has been proposed to function as a Ca^{2+} sensor that regulates synaptic vesicle exocytosis, whereas the soluble *N*-ethylmaleimide-sensitive factor attachment protein receptor (SNARE) complex is thought to form the core of a conserved membrane fusion machine. Little is known concerning the functional relationships between synaptotagmin and SNAREs. Here we report that synaptotagmin can facilitate SNARE complex formation *in vitro* and that *synaptotagmin* mutations disrupt SNARE complex formation *in vivo*. Synaptotagmin oligomers efficiently bind SNARE complexes, whereas Ca^{2+} acting via synaptotagmin triggers cross-linking of SNARE complexes into dimers. Mutations in *Drosophila* that delete the C2B domain of synaptotagmin disrupt clathrin AP-2 binding and endocytosis. In contrast, a mutation that blocks Ca^{2+}-triggered conformational changes in C2B and diminishes Ca^{2+}-triggered synaptotagmin oligomerization results in a postdocking defect in neurotransmitter release and a decrease in SNARE assembly *in vivo*. These data suggest that Ca^{2+}-driven oligomerization via the C2B domain of synaptotagmin may trigger synaptic vesicle fusion via the assembly and clustering of SNARE complexes.

Key words: exocytosis; synaptotagmin; SNARE; Ca^{2+}; synaptic vesicle; membrane fusion; C2 domain; Drosophila

Neuronal exocytosis is precisely controlled by Ca^{2+} ions (Katz, 1969) and is extremely rapid (Llinas et al., 1981). The speed of exocytosis dictates that a small number of molecular rearrangements couple Ca^{2+} influx to the catalysis of bilayer fusion. Recent studies have established that cycles of Ca^{2+}-triggered exocytosis require the assembly and disassembly of the soluble *N*-ethylmaleimide-sensitive factor attachment protein receptor (SNARE) complex (Söllner et al., 1993; Littleton et al., 1998) (for review, see Rothman, 1994; Scheller, 1995; Jahn and Südhof, 1999). In synapses, this complex is composed of the target membrane SNAREs (t-SNAREs) syntaxin (Bennett et al., 1992) and synaptosomal associated protein of 25 kDa (SNAP-25) (Oyler et al., 1989), and the vesicle membrane SNARE (v-SNARE) synaptobrevin/vesicle-associated membrane protein (VAMP) (Trimble et al., 1988). The core of the ternary complex (Fasshauer et al., 1998; Poirier et al., 1998a) is a parallel four-helix bundle (Sutton et al., 1998) that, upon assembly, brings the vesicle and target membranes together, potentially driving bilayer fusion (Poirier et al., 1998b; Hanson et al., 1997; Sutton et al., 1998). Consistent with this model, SNAREs reconstituted into proteoliposomes can assemble and catalyze membrane fusion *in vitro* (Weber et al., 1998).

Although there is evidence that the SNARE complex serves as the core of the fusion machinery, it is unclear how SNARE-mediated fusion is regulated by Ca^{2+}. The synaptic vesicle protein synaptotagmin I (Matthew et al., 1981; Perin et al., 1990) binds Ca^{2+} (Brose et al., 1992) and has been shown, via genetic studies, to be essential for efficient and rapid excitation–secretion coupling *in vivo* (Littleton et al., 1993, 1994; Nonet et al., 1993; DiAntonio and Schwarz, 1994; Geppert et al., 1994). Whether this effect is attributable to a loss of Ca^{2+} sensing (Geppert et al., 1994; Littleton et al., 1994), failure of vesicles to be recycled (Jorgensen et al., 1995), failure to dock efficiently at release sites (Reist et al., 1998), failure of the release machinery to be sequestered near Ca^{2+} channels (Sheng et al., 1997), or combinations of these defects in knock-out animals, remains the subject of debate. However, mutations in *synaptotagmin* can alter the $[Ca^{2+}]$–response curve for secretion (Littleton et al., 1994), and disruption of the *synaptotagmin I* gene in mice selectively inhibits the fast synchronous component of exocytosis (Geppert et al., 1994). Furthermore, the equilibrium and kinetic Ca^{2+}-binding properties of synaptotagmin are consistent with the Ca^{2+} requirement and speed of secretion (Davis et al., 1999). These data support a model in which synaptotagmin functions as a Ca^{2+} sensor for secretion, albeit via an unknown mechanism.

Synaptotagmin spans the vesicle membrane once and binds Ca^{2+} via two C2 domains designated C2A and C2B (Südhof and Rizo, 1996; Desai et al., 2000). One way to better define the function of synaptotagmin would be to generate animals that are selectively defective in the Ca^{2+}-sensing ability of each C2 domain. Here, we use a genetic approach to determine whether the

Received Oct. 9, 2000; revised Nov. 16, 2000; accepted Dec. 11, 2000.

This work was supported by National Institutes of Health Grants GM 56827–01, GM43100, NS40296–01, and NS15390, American Heart Association Grant 9750326N, and the Milwaukee Foundation. J.T.L. was sponsored through a Merck Helen Hay Whitney Foundation fellowship, and E.R.C. is a fellow of the Pew Charitable Trust. We thank R. Jahn, S. Engers, and H. Jackle for generous gifts of antibodies, A. Brunger, G. Schiavo, T. Südhof, R. Scheller, and M. Wilson for cDNA clones, D. Fasshauer for purified SNARE complexes, R. Roy for assistance with experiments, and D. Gaston for molecular modeling.

Correspondence should be addressed to Edwin R. Chapman, Department of Physiology, SMI 129, University of Wisconsin, 1300 University Avenue, Madison, WI 53706. E-mail: chapman@physiology.wisc.edu.

Ca^{2+}-sensing ability of the C2B domain of synaptotagmin functions in synaptic transmission. Furthermore, we investigate the biochemical relationship between synaptotagmin and SNARE dynamics and propose a molecular model by which synaptotagmin may regulate SNARE-catalyzed membrane fusion.

MATERIALS AND METHODS

Individual recombinant proteins. cDNA encoding rat synaptotagmin I (Perin et al., 1990; Osborne et al., 1999) and human SNAP-25B (Bark and Wilson, 1994) were kindly provided by T. C. Südhof (Dallas, TX), G. Schiavo (London, UK), and M. Wilson (Albuquerque, NM), respectively. cDNA encoding rat syntaxin 1A (Bennett et al., 1992) and synaptobrevin II/VAMP II (Elferink et al., 1989) were kindly provided by R. Scheller (Stanford, CA). Soluble forms of syntaxin, SNAP-25B, and synaptobrevin were prepared by subcloning into pTrcHisA (Invitrogen, San Diego, CA), resulting in fusion proteins with T7 and His6 tags at their N termini. His-tagged proteins were expressed and purified as described (Chapman et al., 1995, 1996). Wild-type, *AD1,* and *AD3* mutant rat and *Drosophila* synaptotagmins were generated by PCR, subcloned into pGEX-2T, expressed, purified, and cleaved from the GST-fusion moiety with thrombin, as described (Chapman et al., 1996). All constructs were confirmed by DNA sequencing.

There are two reported rat synaptotagmin I sequences: one with a aspartate at position 374 (D374; Perin et al., 1990) and another with a glycine at this position (G374; Osborne et al., 1999). We have confirmed that both forms of synaptotagmin are expressed in rats and have observed that the G374, but not the D374, form clusters in response to Ca^{2+} (Davis et al., 1999; Desai et al., 2000). The basis for this sequence variability is under investigation. To simplify interpretation of synaptotagmin-SNARE coimmunoprecipitation experiments, the D374 form was used. In the assembly experiments shown in Figure 2, the D374 form was used, but similar results were observed with the G374 form as well as with the AD3 mutant (data not shown). The G374 form was used in the oligomerization assays shown in Figure 3.

Midi SNARE complexes. Midi SNARE complexes were composed of residues 180–262 of syntaxin 1A, full-length SNAP-25A, and residues 1–96 of synaptobrevin II. The components used to assemble midi complexes differ from those used in all other experiments. To obtain high level expression of SNAP-25, rat SNAP-25A was subcloned into the vector pET28a (Novagen, Madison, WI) via *Nhe*I and *Xho*I restriction sites resulting in an N-terminal His6-tag. In addition, four cysteines (cys 84, 85, 90, and 92) were replaced with serines using the overlapping primer method (Chapman and Jahn, 1994). These mutations facilitated expression and purification and had no apparent effects on the structure or binding properties of SNAP-25 (Fasshauer et al., 1999). The cytoplasmic domain of synaptobrevin II was generated as described (Fasshauer et al., 1997), and syntaxin fragment 180–262 was expressed using pET15b. SDS-resistant midi–SNARE complexes were assembled and purified to homogeneity as described (Fasshauer et al., 1997, 1998).

Immunoprecipitation and antibodies. Mouse monoclonal antibodies directed against rat synaptotagmin I (41.1), syntaxin (HPC-1), SNAP-25 (71.2), and synaptobrevin (69.1) were kindly provided by S. Engers and R. Jahn (Göttingen, Germany), and the anti-T7 tag antibody was from Novagen. Monoclonal antisera against *Drosophila* syntaxin (8C3) was used at 1:2000, polyclonal DSYT2 against *Drosophila* synaptotagmin I at 1:2000 (Littleton et al., 1993), and polyclonal anti-*Drosophila* α-adaptin at 1:2000 (Gonzalez-Gaitan et al., 1996).

All immunoprecipitation and bead-binding experiments were performed at 4°C. Immunoprecipitation of recombinant SNAREs and SNARE complexes was performed as described (Chapman et al., 1995). Briefly, recombinant individual SNAREs or SNARE complexes were incubated with recombinant synaptotagmin in Tris-buffered saline (TBS; 20 mM Tris, pH 7.4, 150 mM NaCl) plus 0.5% Triton X-100 in the presence of 2 mM EGTA or 1 mM Ca^{2+} for 2 hr. Syntaxin, synaptobrevin, or SNAP-25 was immunoprecipitated by incubating the samples with HPC-1 (5 μl), 69.1 (1.5 μl), or 71.1 (5 μl) ascites, respectively, for 2 hr and 12 μl of Protein G Sepharose Fast-flow (Amersham Pharmacia Biotech) for 1 hr. The immunoprecipitates were washed three times and analyzed by SDS-PAGE and either immunoblotting or staining with Coomassie blue. As a control for nonspecific precipitation of synaptotagmin, samples were also prepared lacking SNAREs. In each case, the immunoprecipitating antibodies did not bind synaptotagmin, and, under the conditions of the binding assays, synaptotagmin did not precipitate in the absence of SNAREs. Thus, for experiments shown in the Figures (−SNARE) samples also lacked immunoprecipitating antibodies. Coimmunoprecipitation of synaptotagmin was quantified using a Bio-Rad (Hercules, CA) GS-670 Imaging Densitometer. Generation of *Drosophila* head homogenates for AP-2 binding assays was as previously described (Littleton et al., 1998).

[Ca^{2+}] determination. For Ca^{2+} titration experiments, $[Ca^{2+}]_{free}$ was determined using a Microelectrode MI-600 Ca^{2+} electrode, MI-402 microreference electrode (Bedford, NH), and World Precision Instruments (Sarasota, FL) Ca^{2+} standards (pCa^{2+} range of 1–8). Ca^{2+} concentrations <100 μM were buffered using 2 mM EGTA.

In vitro *assembly of SDS-resistant 7S SNARE complexes.* His6-tagged synaptobrevin II (1–96), SNAP-25B (1–206), and syntaxin 1A (1–265) were incubated at 0.5 μM with constant mixing for 0, 5, 15, or 120 min at 25°C with or without 2 μM recombinant cytoplasmic domain of synaptotagmin Ia. All assembly reactions were performed using freshly purified proteins in 150 μl of TBS supplemented with either 2 mM EGTA, 1 mM Mg^{2+}, or 1 mM Ca^{2+}. In some experiments, assembly was performed in the presence of 1 mM DTT. Assembly reactions were stopped by adding 15 μl of 3× SDS sample buffer, containing 10% β-mercaptoethanol, to 30 μl of the reaction mixture. Samples were loaded onto discontinuous 9–15% SDS-PAGE mini-gels (Bio-Rad) without boiling (except where indicated) and separated at 15 mA per gel. The gels were immunoblotted using monoclonal antibodies directed against syntaxin, synaptobrevin, or synaptotagmin; immunoreactive bands were visualized using enhanced chemiluminescence. Synaptotagmin consistently enhanced 7S assembly, but this effect was variable, ranging from 1.5- to 4-fold. A representative experiment showing a threefold enhancement at 5 min is shown in Figure 2*A*.

Interaction of synaptotagmin oligomers with midi–SNARE complexes. Fifteen micrograms of GST-tagged synaptotagmin (amino acids 96–421; G374-version) immobilized on beads was incubated with 10 μM soluble synaptotagmin (amino acids 96–421; G374-version) for 1.5 hr in 150 μl of HEPES-buffered saline (HBS; 50 mM HEPES, pH 7.4, 100 mM NaCl) plus 0.5% Triton X-100 in either 2 mM EGTA or 1 mM Ca^{2+}. Beads were washed three times in binding buffer plus 2 mM EGTA or 1 mM Ca^{2+}, and then incubated with 2 μM midi–SNARE complex for 1.5 hr. Beads were washed three times as described above, and 25% of the samples were subjected to SDS-PAGE; gels were stained with Coomassie blue.

To determine whether SNARE complexes can inhibit the binding of soluble synaptotagmin to immobilized synaptotagmin, oligomerization assays were performed as described above. However, free soluble synaptotagmin was not removed by washing, and the concentration of SNARE complex was titrated (1, 3, and 6 μM). For analysis, samples were boiled, separated by SDS-PAGE, bound synaptotagmin was visualized by staining with Coomassie blue, and SNAREs were detected by immunoblot analysis.

Isolation of Drosophila *SNARE complexes.* Flies of the indicated genotype were frozen in liquid nitrogen, vortexed, and 10 heads for each genotype were homogenized in 50 μl of SDS sample buffer on ice. The samples were briefly centrifuged to pellet cuticle, and 20 μl of the supernatant was resuspended in 30 μl of SDS sample buffer. Samples were loaded onto discontinuous 9 and 15% SDS-PAGE gels without boiling and separated at 15 mA per gel. The gels were immunoblotted with anti-syntaxin monoclonal antibody 8C3 at 1:2000 dilution. Immunoreactive bands were visualized using ECL.

EM. Transmission electron microscopy quantification at photoreceptor synapses was done as previously described (Littleton et al., 1998). The number of vesicles per T-bar was determined by counting vesicles that were under the arms of an active zone T-bar and within 40 nM of the presynaptic membrane. Error measurements are reported in SD.

Drosophila *genetics.* Flies were cultured on standard medium at 23°C.

RESULTS

Synaptotagmin drives SNARE complex assembly, and Ca^{2+}-synaptotagmin drives the cross-linking of SNARE complexes into dimers

To define the biochemical relationship between synaptotagmin activity and SNARE complex assembly, we undertook a detailed analysis of the interaction dynamics between these two essential elements of the vesicle fusion machinery. Direct interactions between synaptotagmin and t-SNAREs have been previously demonstrated; synaptotagmin binds, in a stoichiometric and Ca^{2+}-promoted manner, to both syntaxin and SNAP-25 (Chapman et al., 1995; Schiavo et al., 1997; Davis et al., 1999; Gerona

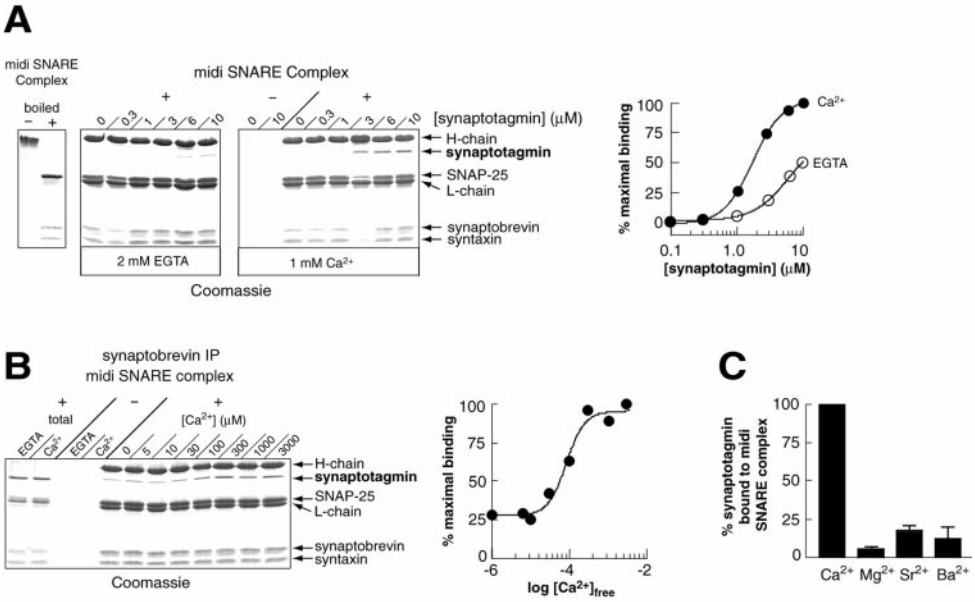

Figure 1. Interaction of synaptotagmin with assembled SNARE complexes. *A, Left panel,* The "midi" SNARE complex is SDS-resistant. Midi SNARE complex (1.5 μg) was dissociated into its component parts (residues 1–96 of synaptobrevin, 1–206 of SNAP-25, and 180–262 of syntaxin) by boiling in SDS sample buffer. *Middle panels,* Increasing concentrations of synaptotagmin were incubated with midi complexes (2 μM) in the presence of EGTA or Ca^{2+} in a 75 μl reaction volume. Synaptotagmin binding was assayed by coimmunoprecipitation using anti-synaptobrevin antibodies. Proteins were separated by SDS-PAGE and visualized with Coomassie blue. Forty percent of the bound material was loaded onto the gel. *Right panel,* Coimmunoprecipitated synaptotagmin was quantified by densitometry. The level of binding in EGTA (*open circles*) and Ca^{2+} (*closed circles*) was normalized to the maximum level of binding and plotted versus [synaptotagmin]. In the presence of Ca^{2+}, the EC_{50} was 1.7 μM; at saturation the stoichiometry was 0.5 mol of synaptotagmin per mole of midi complex. *B, Left panel,* Synaptotagmin (3 μM) was mixed with midi–SNARE complex (2 μM) in 75 μl of HBS–0.5% Triton X-100 plus EGTA (2 mM) or the indicated concentration of Ca^{2+} for 2 hr at 4°C. SNARE complexes were immunoprecipitated with an anti-synaptobrevin antibody. Proteins were separated by SDS-PAGE and stained with Coomassie blue. Forty percent of the bound material was loaded onto the gel; *total* corresponds to 10% of the binding reaction. *Right panel,* Coimmunoprecipitated synaptotagmin was quantified by densitometry, normalized, and plotted versus the free Ca^{2+} concentration. The $[Ca^{2+}]_{1/2}$ was ~100 μM. *C,* Synaptotagmin-midi–SNARE complex formation was monitored as described in *B* in the presence of the indicated divalent cations (1 mM Mg^{2+}; 200 μM Ca^{2+}, Ba^{2+}, Sr^{2+}). The synaptotagmin and midi–SNARE complex concentrations were 2 μM. Synaptotagmin binding was normalized (binding in 2 mM EGTA and 200 μM Ca^{2+} were set at 0 and 100% binding, respectively), and the means from triplicate determinations are plotted. Error bars represent the SD from triplicate determinations.

et al., 2000). To further explore the interaction of synaptotagmin with SNAREs, we assembled syntaxin and SNAP-25 with synaptobrevin to form SDS-resistant ternary SNARE complexes. Because synaptotagmin binds solely to the H3-domain of syntaxin (Chapman et al., 1995; Kee and Scheller, 1996; Davis et al., 1999), we used "midi" SNARE complexes composed of residues 180–263 of syntaxin 1A, full-length SNAP-25A, and residues 1–96 of synaptobrevin II. Assembly of the midi complex is confirmed in Figure 1*A* (*left panel*), where the complex runs at ~67 kDa on SDS polyacrylamide gels and, after boiling, dissociates into the three individual SNARE proteins. Midi complexes were incubated with increasing concentrations of recombinant rat synaptotagmin in either EGTA or Ca^{2+} and then immunoprecipitated with anti-synaptobrevin antibodies. Immunoprecipitates were boiled and analyzed by SDS-PAGE and Coomassie staining. As shown in Figure 1*A* (*middle* and *right panels*), synaptotagmin bound to midi complexes in both EGTA and in Ca^{2+}. Under these conditions, Ca^{2+} increased the affinity of synaptotagmin for the midi complex by approximately an order of magnitude. In the presence of Ca^{2+}, the EC_{50} for synaptotagmin binding to SNARE complexes was 1–2 μM. At saturation, the stoichiometry was 0.5 moles of synaptotagmin per mole of complex, suggesting that one copy of synaptotagmin binds two copies of the SNARE complex. Furthermore, the $[Ca^{2+}]_{1/2}$ for the interaction of synaptotagmin with the SNARE complex was ~100 μM Ca^{2+} (Fig. 1*B*), consistent with the Ca^{2+} dependence for secretion in retinal bipolar neurons (194 μM Ca^{2+}; Heidelberger et al., 1994) and within a factor of 10 of the Ca^{2+} dependence for secretion at the calyx of Held (10–20 μM Ca^{2+}; Bollman et al., 2000; Schneggenburger and Neher, 2000). Binding was selectively promoted by Ca^{2+} versus other divalent cations (Fig. 1*C*).

Isolated t-SNAREs have a distinct and less ordered conformation than t-SNAREs that are assembled into the four helix bundle that constitutes the core of the SNARE complex (Fasshauer et al., 1997; Sutton et al., 1998; Fiebig et al., 1999). The observation that synaptotagmin binds to isolated t-SNAREs, as well as to assembled SNARE complexes, efficiently and in a Ca^{2+}-regulated manner, indicates that isolated t-SNAREs are ordered into their ternary "SNARE-complex conformations" after complex formation with synaptotagmin. This model predicts that synaptotagmin, via its "ordering" of t-SNAREs, would facilitate assembly of SNARE complexes. To test this prediction, we incubated purified SNAREs (syntaxin, SNAP-25, and synaptobrevin) with and without rat synaptotagmin in the presence and absence of Ca^{2+}, for increasing periods of time. SDS-resistant SNARE complexes were detected using antibodies directed against syntaxin (Fig. 2*A*), synaptobrevin (Fig. 2*C*), or SNAP-25 (data not shown). These complexes were disassembled into monomeric SNAREs after boiling in SDS (Fig. 2*A,C*). Consistent with previous reports, SDS-resistant SNARE complexes formed in the absence of synaptotagmin and Ca^{2+} (Fig. 2*A*; Hayashi et al., 1994). Under these conditions, Ca^{2+} had no apparent effect on the rate or extent of SDS-resistant SNARE complex assembly. However, addition of synaptotagmin to mixtures of isolated SNAREs accelerated SNARE complex assembly (Fig. 2*A,B*). This effect is marked at early time points; at 5 min, synaptotagmin drove a threefold enhancement of SNARE complex assembly, and by 120 min equal amounts of SNARE complex accumulated in the presence and absence of synaptotagmin (Fig. 2*C*). Surprisingly, the ability of synaptotagmin to drive complex assembly was Ca^{2+}-independent, despite the fact that Ca^{2+} promotes binding of synaptotagmin to t-SNAREs. Therefore, in addition to the kinetics experiments shown in Figure 2*A*, we also conducted synaptotagmin-titration experiments. In all kinetic and titration experiments, the ability of synaptotagmin to enhance the rate of SNARE complex assembly was independent of Ca^{2+} (data not

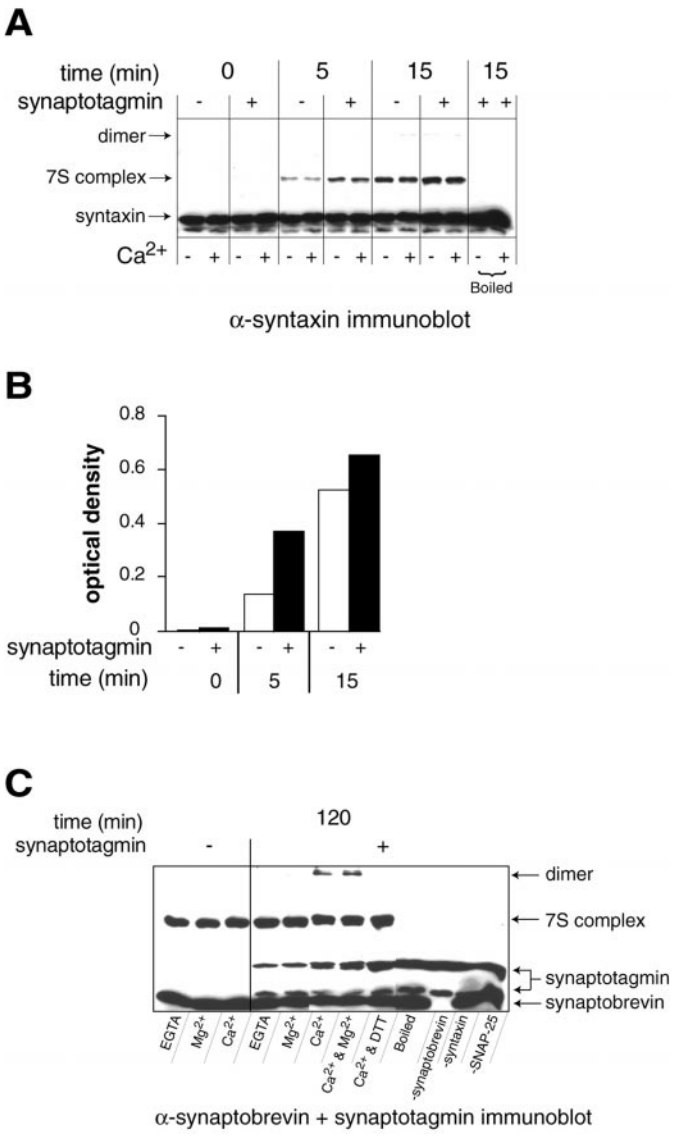

Figure 2. Synaptotagmin facilitates SNARE complex assembly *in vitro*. *A,* Recombinant his6-syntaxin, his6-SNAP-25B, and his6-synaptobrevin were incubated in the presence and absence of recombinant synaptotagmin in 2 mM EGTA ($-Ca^{2+}$) or 1 mM Ca^{2+} ($+Ca^{2+}$) for 0, 5, or 15 min at room temperature. SDS-resistant 7S SNARE-complex formation was assayed by subjecting the samples to SDS-PAGE, without previous boiling (except where indicated), and immunoblotting with anti-syntaxin antibodies. Immunoreactive bands were visualized using enhanced chemiluminescence. *7S* denotes an SDS-resistant complex consisting of syntaxin, SNAP-25, and synaptobrevin. *dimer* denotes the trace formation of disulfide-bonded SNARE complex dimers that form under these conditions. *B,* The optical densities of 7S complexes from the $+Ca^{2+}$ lanes in *A* are plotted versus time of incubation. *C,* Assembly experiments were performed as described in *A* for 2 hr but in the absence of DTT, except where indicated. Assembly reactions were conducted with (+) or without (−) synaptotagmin in either 2 mM EGTA, 1 mM Mg^{2+}, 1 mM Ca^{2+}, or 1 mM Mg^{2+} plus 1 mM Ca^{2+}. As controls, samples were prepared that lacked either synaptobrevin, syntaxin, or SNAP-25. As a further control, samples were boiled before analysis. Samples were analyzed by immunoblotting with a mixture of anti-synaptobrevin and anti-synaptotagmin antibodies. Ca^{2+} and synaptotagmin enhanced the formation of SDS-resistant dimers. These dimers are disulfide-linked and are dissociated by DTT. SDS-resistant 7S complex formation only occurs in the presence of all three SNAREs, and complexes are dissociated by boiling.

shown). The reason for this lack of a Ca^{2+}-effect is unclear. One possibility is that the difference in affinity of synaptotagmin for SNAREs in the presence and absence of Ca^{2+} is not great enough to yield differences under the conditions of our assembly experiments where we measured assembly on minute rather than millisecond time scales. However, we observed that Ca^{2+}-synaptotagmin can trigger the formation of SDS-resistant SNARE complex dimers (Fig. 2*C*). These dimers result from intermolecular disulfide bonds that can be disrupted by DTT (Fig. 2*C*). Thus, Ca^{2+} can act via synaptotagmin to drive the "cross-linking" of two SNARE complexes together. These findings are congruent with the estimated stoichiometry of one synaptotagmin bound to two SNARE complexes as described in Figure 1*A*. We note that in some experiments, Ca^{2+} alone was able to trigger low levels of cross-linked dimer formation, perhaps via direct effects on the SNARE complex (Sutton et al., 1998). However, in all experiments, this effect was markedly enhanced by the addition of synaptotagmin. Furthermore, cross-linking is specifically driven by Ca^{2+}-synaptotagmin, 1 mM Mg^{2+} does not trigger cross-linking, nor does it inhibit Ca^{2+}–synaptotagmin-driven cross-linking (Fig. 2*C*). Control experiments demonstrated that the dimers were composed of all three SNAREs; omission of any of the SNAREs precluded dimer formation (Fig. 2*C*), and dimers were recognized by antibodies directed against each component of the SNARE complex (Fig. 2*A,C*; data not shown). In summary, these data indicate that Ca^{2+}, acting via synaptotagmin, can drive conformational changes in SNARE complexes that result in the formation of cross-linked SNARE complex dimers.

Assembly of synaptotagmin oligomers with SNARE complexes

One prominent feature of the synaptotagmin family is the ability of synaptotagmins to undergo both homo- and hetero-oligomerization in a Ca^{2+}-dependent manner (Sugita et al., 1996; Chapman et al., 1998; Osborne et al., 1999; Desai et al., 2000). This property is conserved from invertebrates to mammals (Littleton et al., 1999; Desai et al., 2000), suggesting it may be essential for the function of synaptotagmin in neurotransmitter release. Given that Ca^{2+}-triggered synaptotagmin self-association occurs on rapid time scales (Davis et al., 1999), one hypothesis is that oligomerization may play an important role in late stages of SNARE assembly and clustering of SNARE complexes into a collar-like fusion pore. If this model is correct, synaptotagmin should be able to oligomerize and bind to SNARE complexes at the same time. To examine this possibility, synaptotagmin was immobilized on beads and assayed for SNARE complex binding activity. We made use of the observation that synaptotagmin, fused to GST, cannot efficiently bind SNARE complexes. After removal of the GST moiety, high-affinity complexes between synaptotagmin and SNARE complexes are efficiently assembled (Chapman et al., 1996). This result is shown in Figure 3*A*, where the immobilized GST–synaptotagmin fusion protein bound SNARE complexes only weakly in both the absence and presence of Ca^{2+} (Fig. 3*A*). We then assembled soluble synaptotagmin onto immobilized GST–synaptotagmin by virtue of the Ca^{2+}-triggered clustering activity of the protein. Unbound synaptotagmin was removed by washing, and the ability of the synaptotagmin-GST–synaptotagmin oligomer was assayed for SNARE complex binding activity. As shown in Figure 3*A*, oligomerized synaptotagmin efficiently captured assembled SNARE complexes.

As a further test of the model in which synaptotagmin oli-

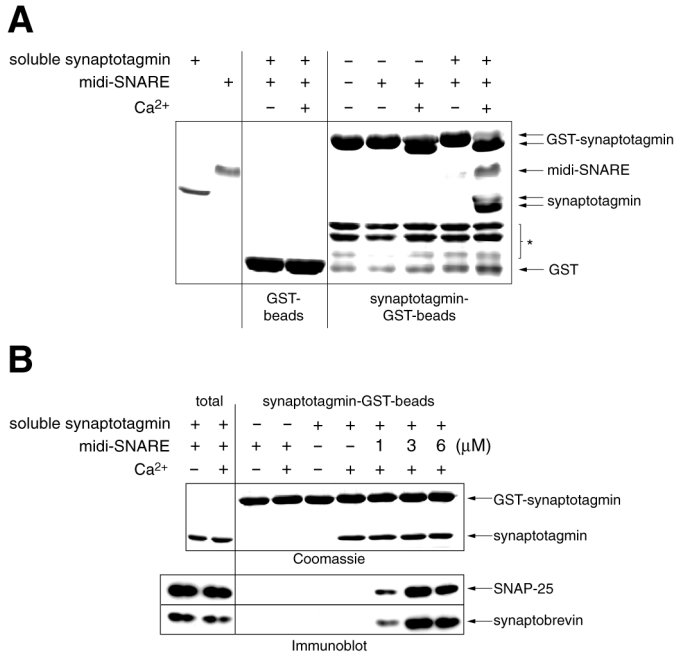

Figure 3. Oligomerized synaptotagmin binds to assembled SNARE complexes. *A,* GST and GST–synaptotagmin were immobilized on beads (15 μg per data point) and assayed for binding to midi–SNARE complexes (2 μM) in 2 mM EGTA ($-Ca^{2+}$) or 1 mM Ca^{2+} ($+Ca^{2+}$) in 150 μl of HBS using a cosedimentation assay, as described in Materials and Methods. To leave SNARE complexes intact, samples were subjected to SDS-PAGE without previous boiling. Coomassie staining revealed only low levels of SNARE binding to immobilized synaptotagmin in either condition. Immobilized synaptotagmin was then preincubated with soluble synaptotagmin (10 μM) in EGTA or Ca^{2+}. Beads were washed three times to remove unbound soluble synaptotagmin, and the soluble- immobilized synaptotagmin oligomers were assayed for binding to midi–SNARE complexes. Twenty-five percent of the bound material was loaded onto the gel; the *left two lanes* correspond to 0.3 and 0.5 μg of soluble synaptotagmin and midi–SNARE complex, respectively. Coomassie staining revealed efficient binding of soluble synaptotagmin to immobilized synaptotagmin. Furthermore, midi–SNARE complexes efficiently bound to the soluble-immobilized synaptotagmin oligomers. These results demonstrate that synaptotagmin, which has oligomerized, is capable of binding SNARE complexes. *Denotes proteolytic fragments from GST–synaptotagmin. Note, Ca^{2+} induces a shift in the mobility of synaptotagmin that has not been boiled. Therefore, soluble and GST–synaptotagmin are indicated with *double arrows*. *B,* SNARE complexes do not inhibit synaptotagmin oligomerization. GST (12 μg per data point) and GST–synaptotagmin (8 μg per data point) were immobilized on beads. Soluble synaptotagmin (1.5 μM; +) and midi–SNARE complex (6 μM; +) or the indicated [SNARE complex] were incubated with the beads in 2 mM EGTA (−) or 1 mM Ca^{2+} (+) for 1.5 hr. Samples were also prepared that lacked SNARE complexes (−) or soluble synaptotagmin (−). Bound material was boiled in SDS sample buffer and subjected to SDS-PAGE. Twenty-five percent of the bound material was loaded onto the gel; total corresponds to the mixture of 0.3 and 0.7 μg of soluble synaptotagmin and midi–SNARE complex. Gels were stained with Coomassie blue to visualize bound synaptotagmin. Staining of disassembled SNARE complexes was poor, therefore SNARE binding was detected by immunoblotting with anti-SNAP-25 and anti-syntaxin antibodies. Immunoreactive bands were visualized using enhanced chemiluminescence.

gomerizes and binds to SNAREs at the same time, we determined whether SNARE complexes act as competitive inhibitors of synaptotagmin oligomerization. For these experiments we monitored the Ca^{2+}-dependent binding of soluble synaptotagmin to immobilized synaptotagmin in the presence of increasing concentrations of SNARE complexes. As shown in Figure 3*B*, addition of SNAREs did not impede oligomerization. Our biochemical observations are consistent with a role for synaptotagmin oligomerization and SNARE binding in triggering vesicle fusion. To directly test this model, we characterized mutations in *Drosophila* synaptotagmin I that block Ca^{2+}-dependent oligomerization.

The C2B domain of synaptotagmin is required for both exocytosis and endocytosis of synaptic vesicles *in vivo*

A collection of 20 different alleles of *synaptotagmin I* (*syt*) have been generated in *Drosophila* (Littleton et al., 1993, 1994; DiAntonio and Schwarz, 1994), providing useful experimental material to determine the mechanism by which synaptotagmin functions in synaptic vesicle cycling. Many of these mutations in *syt*, including P-element insertions, enhancer/promoter deletions, and early stop codons in the open reading frame (DiAntonio and Schwarz, 1994; Littleton et al., 1994), disrupt synaptic function by decreasing the levels of wild-type synaptotagmin at synapses. However, several *syt* alleles display intragenic complementation (Littleton et al., 1994). This form of complementation is often observed for genes that encode proteins that are part of multimeric complexes and that contain multiple distinct functional domains. Thus, intragenic complementation for *syt* mutations suggests the presence of several independent domains within synaptotagmin that mediate distinct steps in neurotransmitter release. Two of the *syt* alleles involved in intragenic complementation are *AD1* and *AD3.* Flies containing various heteroallelic combinations with *AD1* and *AD3* display defects including a severe lack of coordination and dramatically decreased viability. Previous electrophysiological analysis of heteroallelic combinations involving *AD1* and *AD3* (Littleton et al., 1994) demonstrated a profound decrease in synaptic exocytosis. At low Ca^{2+} concentrations, evoked release is virtually abolished in *AD3* mutants. By raising extracellular Ca^{2+} to 6 mM, exocytosis in *AD3* mutants can be partially rescued (Fig. 4*C*). In contrast, *AD1* mutants have severe defects in synaptic transmission that cannot be rescued by higher levels of extracellular Ca^{2+} (Fig. 4*C*). In addition, recordings from *synaptotagmin* alleles that are viable with *AD1* (*T7* and *T41*) and *AD3* (*T7, T41, T11, D2, D3, D37, D45*) show either the *AD1* or *AD3* phenotype regardless of the other allele with which *AD1* or *AD3* are paired. Indeed, the same *synaptotagmin* mutants (*T41, T7*) behave dramatically different when paired with *AD1* or *AD3*. Thus, the *AD1* and *AD3* alleles confer the dominant phenotype to any *synaptotagmin* allele with which they are paired (even when paired with the same alleles—*T7, T41*), leading us to focus on the molecular defects in the *AD1* and *AD3* mutants. Immunolocalization studies reveal that the mutant synaptotagmins are targeted to synapses in *AD1* and *AD3* mutants (data not shown). The amount of synaptotagmin that is present at mutant synapses is difficult to quantify precisely because we do not know how these mutations affect the ability of our anti-synaptotagmin I antibody to detect the mutated protein *in vivo*. However, *AD1* and *AD3* mutants over a deletion that completely removes synaptotagmin are far less severe phenotypically than null mutants such as *T77* and *AD4* over deletion (Littleton et al., 1994) and survive much longer as larva than do null mutants. These observations directly demonstrate that the *AD1* and *AD3* mutant synaptotagmin proteins are made and have partial function at synapses, allowing these mutants to survive and function more efficiently than mutants that completely remove synaptotagmin and die as embryos. Thus, an altered func-

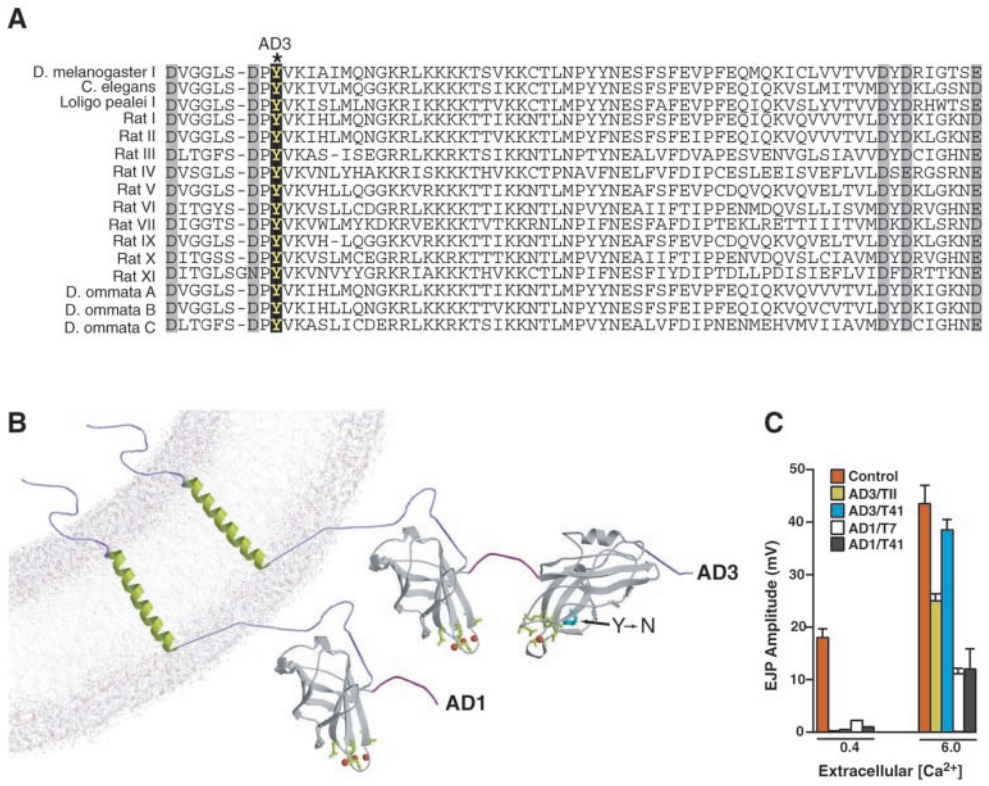

Figure 4. Mutations in the C2B domain of *Drosophila* synaptotagmin I. *A,* Alignment of the C2B domain sequence surrounding the Y364N change found in the *AD3* mutant (DiAntonio and Schwartz, 1994). The five putative Ca^{2+} ligands are highlighted in *gray*, whereas the *AD3* change is indicated in *black*. Y364 is conserved among all synaptotagmin isoforms from *C. elegans* to humans. *B,* Predicted structure of the AD1 and AD3 mutant proteins based on the crystal structure of synaptotagmin III (see Fig. 9 for details). The location of the Y to N change in AD3 is indicated by the *arrow*. The *AD1* mutations result in a premature stop codon deleting the C2B domain. *C,* The electrophysiological defects observed in *AD3* and *AD1* heteroallelic combinations (Littleton et al., 1994) are plotted against the responses of the control *cn bw sp* line. Recordings were made in 0.4 or 6.0 mM Ca^{2+} in Jan's Ringer's solution. Excitatory junctional potential (EJP) amplitude at muscle fiber 6 in segments A3–A5 is plotted vs the extracellular Ca^{2+} concentration. At low Ca^{2+}, both AD1 and AD3 exhibit a profound block in evoked secretion. At higher Ca^{2+} levels, the defects in *AD3* mutants can be partially rescued, whereas *AD1* mutants continue to have dramatically abnormal synaptic responses. These EJP responses have not been corrected for nonlinear summation. Thus, both *synaptotagmin* mutants still have significant defects compared with control responses even in high calcium, where the control responses already saturated at these calcium levels. Dominant defects from the *AD1* and *AD3* alleles when paired with a wild-type allele of synaptotagmin have not been observed (Littleton et al., 1994).

tion of the mutant synaptotagmins, rather than a loss of the protein at synapses, is likely the cause of the electrophysiological defects. We cannot completely rule out some contribution to the phenotype from altered protein levels that are beyond our detection. Sequence analysis of *AD1* and *AD3* revealed that the *AD1* phenotype is caused by a premature stop codon that deletes the C2B domain. *AD3* results from a Y to N substitution in C2B (DiAntonio and Schwarz, 1994) at a residue (364) that is highly conserved in all synaptotagmin isoforms from *Caenorhabditis elegans* to humans (Fig. 4*A*). The crystal structure of the cytoplasmic domain of rat synaptotagmin III (Sutton et al., 1999) indicates that the *AD3* mutation lies near two conserved aspartate residues that may function as Ca^{2+} ligands (Fig. 4*B*). These two mutants allow us to investigate the *in vivo* roles of the C2B domain of synaptotagmin I in synaptic function.

We first examined morphological defects in *AD1* and *AD3* mutants to determine where in the synaptic vesicle cycle each mutant is blocked. For this analysis we examined the first optic neuropil containing 800 highly stereotypic optic cartridges with defined synaptic contacts between photoreceptor axons and laminar neurons that can be readily identified by the presence of presynaptic T-bars. We focused specifically on the histaminergic synapses between photoreceptors (R1–R6) and postsynaptic laminar neurons (L1 and L2). Electroretinogram (ERG) recordings, in which synaptic transmission between photoreceptors and second order neurons in the lamina is indicated by the on and off transients in response to a light flash, revealed that both *AD1* and *AD3* heteroallelic mutants lack these transients (Fig. 5). Thus, these mutations disrupt synaptic transmission at photoreceptor synapses as well as at neuromuscular junctions.

To examine the morphological correlates of the block in synaptic transmission in *AD1* and *AD3*, electron microscopy was performed on the photoreceptor synapses after 10 min of constant light stimulation before fixation to drive continuous vesicle cycling. A total of 168 micrographs were examined from *cn*, *AD1/T41*, *AD1/T7,* and *AD3/T11* flies (n = 3–10 flies for each genotype). The overall architecture of the lamina was normal in *syt* mutants. The most dramatic difference was a decrease ($p < 0.05$, unpaired Student's t test) in the number of synaptic vesicles in photoreceptor terminals of *AD1/T7* and *AD1/T41* mutants compared with controls (*AD1 cn/T41 cn*, 25 + 14 SD; *AD1 cn/T7 cn,* 27 ± 20 SD; *AD3 cn/T11 cn*, 88 ± 28 SD; *cn* controls, 96 ± 37 SD (Fig. 5, compare *A, B*), suggesting a defect in endocytosis in *AD1* heteroallelic mutants. Although we cannot rule out that the loss of synaptic vesicles in *AD1* mutants is caused by a defect in vesicle biogenesis from an internal compartment as opposed to a direct defect in endocytosis, the lack of any vesicle biogenesis defect in *synaptotagmin* null mutants (Reist et al., 1998) argues against this alternative interpretation. In contrast, *AD3* mutants did not have depleted nerve terminals compared with controls, indicating that endocytosis in not disrupted in this mutant. Indeed, synaptic vesicles could be clearly visualized in contact with the presynaptic membrane under T-bars (Fig. 5*C*), indicating that *AD3* mutant vesicles can undergo docking but are defective at a later step in exocytosis (2.6 ± 1.4 SD docked vesicles in *AD3 cn/T11 cn* compared with 2.3 ± 0.9 in *cn* controls).

The morphological and electrophysiological analysis of *AD1* and *AD3* suggest that fundamentally different processes are affected in the two mutants. *AD1* terminals are relatively depleted of synaptic vesicles compared with controls (Fig. 5*B*), and synap-

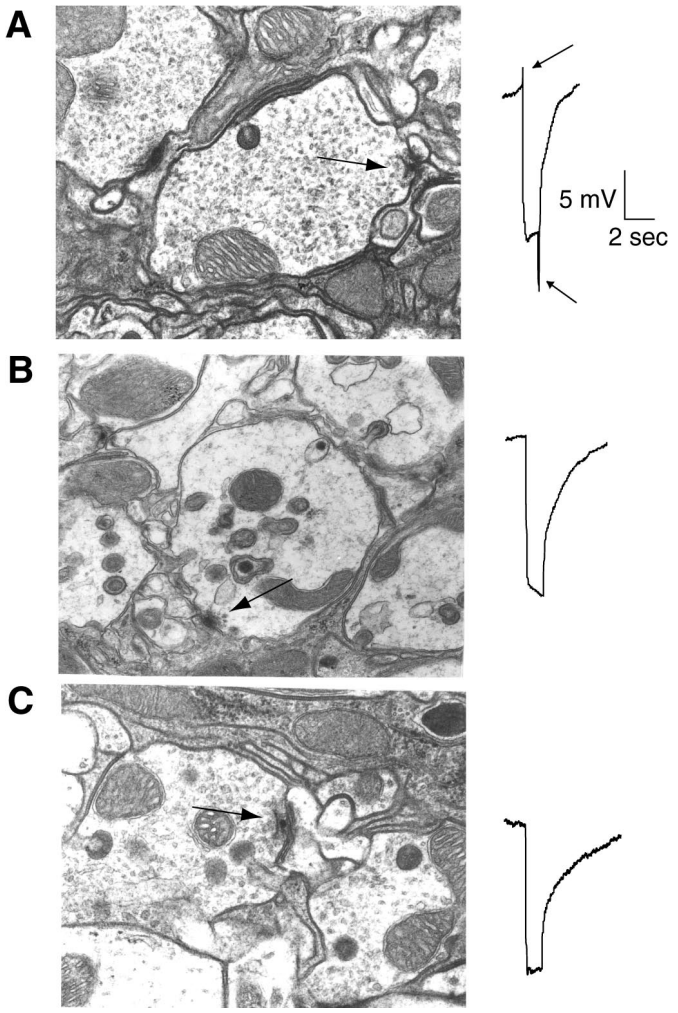

Figure 5. Ultrastructural analysis of stimulated synapses in C2B mutants. Ultrastructural defects in control *cn* (*A*), *AD3 cn/T11 cn* (*B*), and *AD1 cn/T41 cn* (*C*) photoreceptor synapses were examined by driving photoreceptors with constant light stimulation for 10 min, followed by rapid fixation. Both *AD1* and *AD3* mutants lack the on–off transients measured during ERG recordings in the retina (shown on the *right*), demonstrating that synaptic transmission is disrupted at these photoreceptor synapses. *AD1* mutants show a decrease in the overall number of synaptic vesicles, whereas *AD3* synapses do not show a depletion of synaptic vesicles, but rather a defect in the ability of docked synaptic vesicles to fuse. Quantification of vesicles per photoreceptor synapse for each of the genotypes was: *AD1 cn/T41 cn*, 25 ± 14 SD; *AD1 cn/T7 cn,* 27 ± 20 SD; *AD3 cn/T11 cn*, 88 ± 28 SD; *cn* controls, 96 ± 37 SD. Quantification of vesicles per T-bar for each of the genotypes was: *AD1 cn/T41 cn*, 1.4 ± 0.9 SD; *AD1 cn/T7 cn,* 1.9 ± 0.9 SD; *AD3 cn/T11 cn*, 2.6 ± 1.4 SD; *cn* controls, 2.3 ± 0.9 SD.

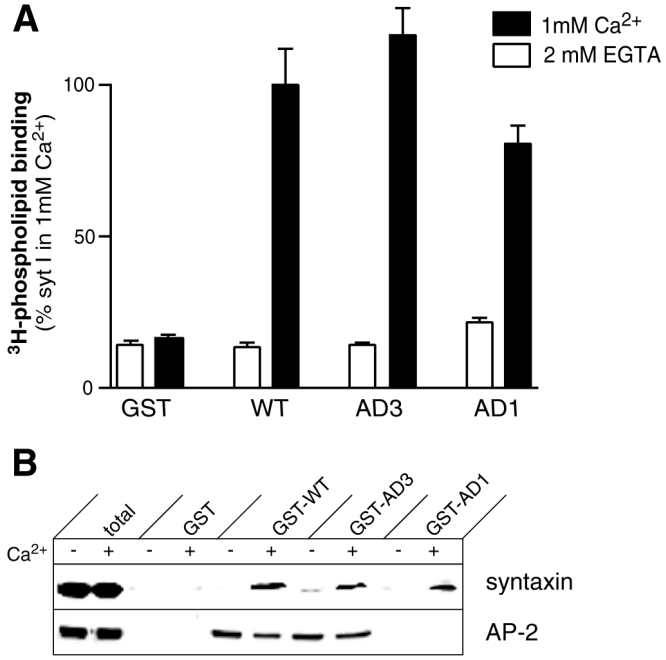

Figure 6. Synaptotagmin AD1 mutants fail to bind AP-2. *A,* Ca^{2+}-dependent phospholipid binding of immobilized recombinant wild-type (*WT*), AD3, or AD1 synaptotagmin I proteins. Both AD1 and AD3 recombinant proteins showed robust Ca^{2+}-stimulated phospholipid binding. Phospholipid binding assays were conducted as previously described (Littleton et al., 1999). *B,* Binding of recombinant syntaxin (5 μM) and native AP-2 α-adaptin (0.2 mg of *Drosophila* head membranes) to 30 μg of recombinant WT, AD3, or AD1 *Drosophila* synaptotagmins in 2 mM EGTA or 1 mM Ca^{2+} for 2 hr at 4°C. For detection of recombinant syntaxin binding to synaptotagmins, Western analysis with the monoclonal anti-syntaxin antisera 8C3 was performed. For analysis of AP-2 binding, fly head membranes were prepared as previously described (Littleton et al., 1998), and AP-2 binding was detected with a polyclonal antibody generated against α-adaptin (Gonzalez-Gaitan and Jackle, 1996). Immunoreactive bands were visualized by enhanced chemiluminescence. Both AD1 and AD3 mutant proteins showed Ca^{2+}-dependent binding to syntaxin. However, only AD3 showed an interaction with AP-2.

tic transmission cannot be rescued by high extracellular Ca^{2+} (Fig. 4*C*). *AD3* mutants have a defect in exocytosis, not endocytosis, (Fig. 5*C*; see Fig. 7*A*), and release can be partially rescued by high extracellular Ca^{2+} (Fig. 4*C*). Thus, the morphologically docked vesicles in *AD3* mutants are also physiologically competent for release but require significantly higher Ca^{2+} concentrations. We therefore examined the biochemical defects caused by *AD1* and *AD3* to determine which activities of the C2B domain are required for endocytosis and exocytosis, respectively. For this analysis we generated GST fusion proteins containing the cytoplasmic domains from wild-type *Drosophila* synaptotagmin, AD1 (C2A domain alone lacking C2B), and AD3. To determine whether AD1 and AD3 are able to penetrate membranes in the presence of Ca^{2+}, we tested the immobilized recombinant cytoplasmic domains for their ability to bind liposomes (25% phosphatidyl serine, 75% phosphatidyl choline) with or without Ca^{2+} (Fig. 6*A*). Wild-type, AD1, and AD3 fusion proteins all showed robust Ca^{2+}-dependent phospholipid binding, an activity previously shown to be mediated by the C2A domain of synaptotagmin Ia (Bai et al., 2000; Desai et al., 2000). We next examined binding to the t-SNARE, syntaxin 1A, whose Ca^{2+} dependence is also mediated by Ca^{2+} ligands in the 2A domain of synaptotagmin Ia (Bai et al., 2000; Desai et al., 2000). Recombinant *Drosophila* syntaxin 1 was able to interact with wild-type, AD1, and AD3 fusion proteins (Fig. 6*B*). We also examined the interaction of synaptotagmin with the clathrin adapter AP-2. Binding of the AP-2 complex from *Drosophila* head extracts was detected with an antibody generated against α-adaptin (Gonzalez-Gaitan et al., 1996). Whereas wild-type and AD3 synaptotagmin bound AP-2 in the absence or presence of Ca^{2+}, AD1 synaptotagmin did not bind AP-2 under either condition (Fig. 6*B*). Thus, as reported for mammalian synaptotagmin I, AP-2 binding to *Drosophila* synaptotagmin is also mediated through the C2B domain (Zhang et al., 1994). We conclude that AP-2 binding to synaptotagmin and subsequent clathrin recruitment is altered in *AD1* mutants, leading to defective endocytosis and a relative depletion of synaptic

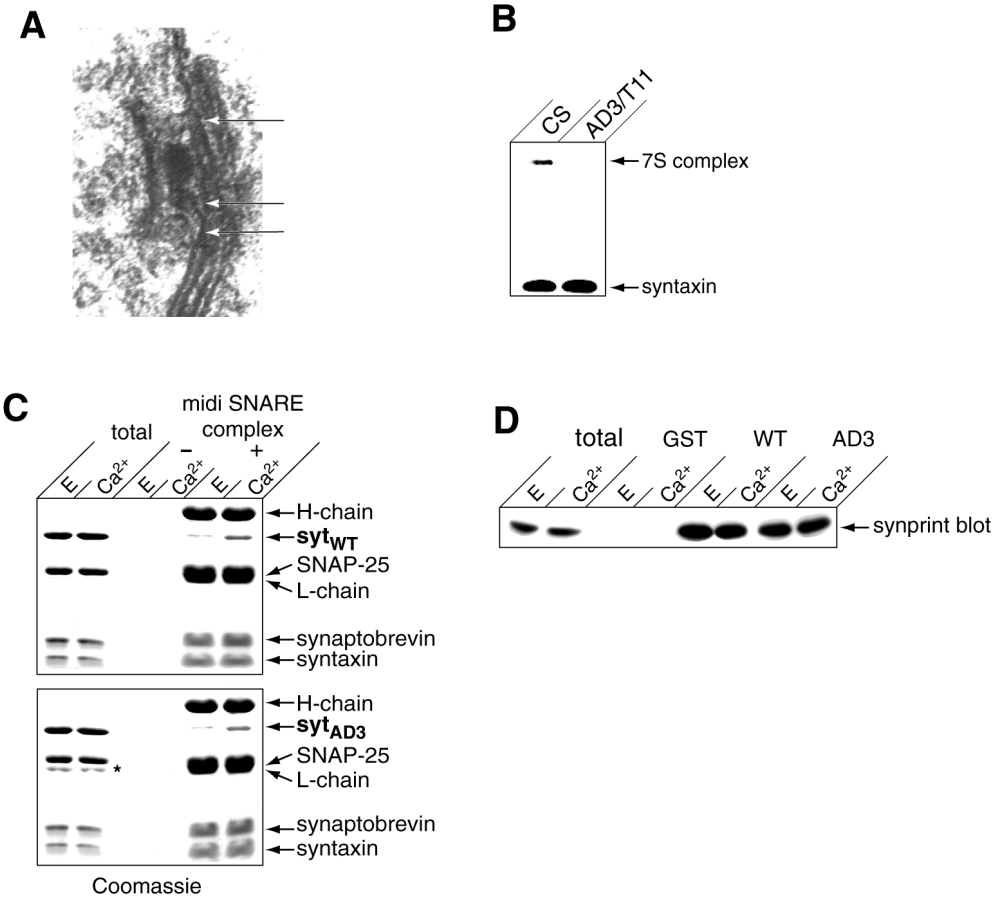

Figure 7. Synaptotagmin AD3 mutants decrease SNARE complex assembly *in vivo*. *A,* Enlarged image of an active zone in *AD3/T11* mutant photoreceptor terminals demonstrating docked vesicles (*arrowheads*) under a T-bar that have not fused. *B,* 7S complexes from 10 control (*CS*) or *synaptotagmin AD3/T11* mutants were isolated. Syntaxin is present in a 35 kDa monomeric form and in a 73 kDa complex with SNAP-25 and synaptobrevin in wild-type flies. A severe reduction in the amount of 7S complex was found in *AD3/T11 synaptotagmin* mutants. *C,* Both wild-type and AD3 recombinant synaptotagmins are able to bind SNARE complexes in a Ca^{2+}-stimulated manner. Either 3 μM wild-type (syt_{WT}) or AD3 mutant synaptotagmin (syt_{AD3}) was incubated with 3 μM midi–SNARE complex for 1.5 hr in either 2 mM EGTA (*E*) or 1 mM Ca^{2+}. Midi–SNARE complex was immunoprecipitated, and samples were separated by SDS-PAGE and stained with Coomassie blue. As a control, samples were prepared that lacked midi–SNARE complex and immunoprecipitating antibodies. Thirty percent of the immunoprecipitated material was loaded onto the gel; total corresponds to 6% of the binding reaction. Note: the *asterisk* indicates a proteolytic fragment present in preparations of soluble AD3 mutant rat synaptotagmin. *D,* Both wild-type and AD3 synaptotagmins are able to bind the mammalian synprint peptide. Ten micrograms of GST or GST fused to the cytoplasmic domain of WT or AD3 mutant synaptotagmin were immobilized on beads and incubated with 1 μM T7-tagged synprint for 2 hr in 2 mM EGTA (*E*) or 1 mM Ca^{2+}. Samples were washed, and bound material was subjected to SDS-PAGE and immunoblot analysis using an anti-T7 tag antibody and enhanced chemiluminescence. Twelve percent of the bound material was loaded onto the gel; total corresponds to 3.5% of the binding reaction.

vesicles in stimulated synapses. Although complete removal of the C2B domain would also be expected to disrupt the exocytotic activities mediated by C2B, the loss of vesicles in the *AD1* mutant dominates the morphological and electrophysiological phenotype. A similar morphological depletion of synaptic vesicles has been observed in a *C. elegans synaptotagmin* mutant that also deletes the C2B domain (Jorgensen et al., 1995). These endocytotic defects preclude the investigation of the role of the C2B domain in exocytosis in AD1 *mutants*. The lack of any defect in AP-2 binding by the *AD3* mutant protein and the corresponding lack of an endocytotic defect by morphological or electrophysiological criteria in *AD3* mutants defines a second function for the C2B domain of synaptotagmin in synaptic vesicle exocytosis that is disrupted in *AD3* mutants.

The AD3 mutation selectively impairs Ca^{2+}-driven conformational changes and Ca^{2+}-triggered oligomerization of the C2B domain of synaptotagmin

Synaptic vesicles in *AD3* mutants are capable of translocating and docking at active zones during synaptic stimulation, as shown in Figure 7*A*. Thus, it is likely that the defect in *AD3* mutants lies somewhere after docking. This interval encompasses both priming and fusion, although it is unknown what molecular events occur during this period. One possibility is that individual SNAREs assemble into various stages of "loose" and "tight" states of SNARE complexes (Xu et al., 1999), generating a potential fusion pore that can be triggered to open by Ca^{2+}. We were thus interested in determining whether there were defects in a specific stage of SNARE assembly in the *AD3* mutant. One possibility is that synaptotagmin is required to trigger SNARE complex assembly. Another possibility is that synaptotagmin binds preassembled SNARE complexes and prevents them from mediating full fusion until arrival of a Ca^{2+} signal. To explore these possibilities, we examined 7S complexes in head extracts of *AD3* mutants. SNARE complexes do not form in SDS (Littleton et al., 1998), but once the complex is formed, they are resistant to dissociation by SDS unless the sample is boiled (Hayashi et al., 1994). To assay complex formation in flies, supernatants from SDS-solubilized control and *AD3* mutant fly heads were separated on SDS-PAGE gels and probed with an anti-syntaxin antiserum. Monomeric 35 kDa syntaxin can be detected, as well as the 73 kDa SNARE complex containing syntaxin, synaptobrevin, and SNAP-25. Because 7S SNARE complexes do not form in SDS, the complex we detect corresponds to that present *in vivo*. *AD3* mutants show a dramatic decrease in the amount of 7S complex (Fig. 7*B*), consistent with a defect in the ability of synaptotagmin to trigger SNARE complex formation rather than a defect in triggering fusion after SDS-resistant SNARE complex assembly. The block in SNARE complex assembly in *AD3* mutants suggests an activity mediated by the C2B domain of synaptotagmin that also acts late in the exocytotic pathway to trigger SNARE assembly and consequent fusion. We therefore under-

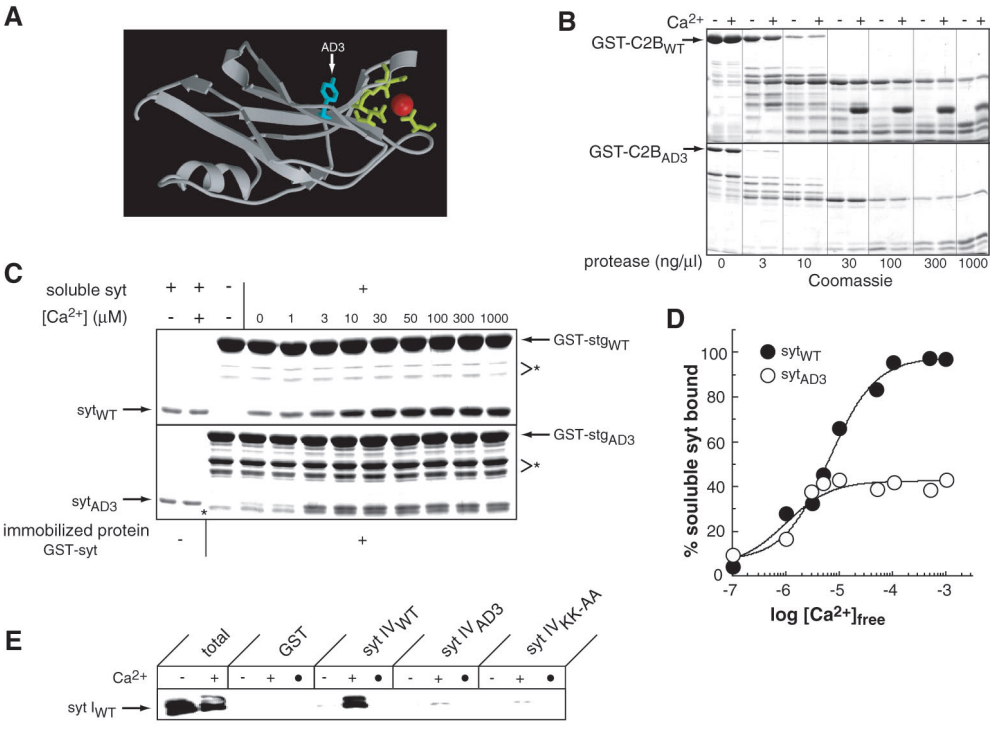

Figure 8. The *AD3* mutation blocks Ca^{2+}-driven conformational changes within the C2B domain of synaptotagmin and disrupts Ca^{2+}-triggered oligomerization activity. *A,* Crystal structure of the C2B domain of synaptotagmin III. This image was modified from Sutton et al. (1999); the structure of the C2B domain of synaptotagmin I has not been reported, however, all known C2B domains share similar structures. The tyrosine that is mutated to an asparagine in the *AD3* mutant allele of *Drosophila* synaptotagmin is indicated, as are five putative Ca^{2+} ligands and a single bound Mg^{2+} ion. *B,* The C2B domain of WT (GST-$C2B_{WT}$) and AD3 (GST-$C2B_{AD3}$) rat synaptotagmin Ib were immobilized as a GST fusion proteins (20 μg/data point) and subjected to limited proteolysis in the presence of 2 mM EGTA (−) or 1 mM Ca^{2+} (+) at the indicated [chymotrypsin] for 60 min at rt. Samples were boiled in SDS sample buffer, analyzed by SDS PAGE, and stained with Coomassie blue. *C,* Ca^{2+}-triggered synaptotagmin oligomerization is impaired by the AD3 mutation. Eight micrograms of GST or GST fused to the cytoplasmic domain of wild-type (syt_{WT}) or AD3 mutant (syt_{AD3}) *Drosophila* synaptotagmin was immobilized on beads. Beads were incubated with 1.5 μM soluble WT or AD3 mutant *Drosophila* synaptotagmin for 1.5 hr in 150 μl of TBS plus 0.5% Triton X-100 and either 2 mM EGTA (−), 1 mM Ca^{2+} (+), or the indicated concentration of Ca^{2+}. Beads were washed three times with binding buffer and boiled in SDS sample buffer. Three percent of the soluble synaptotagmin from the binding assay (*left two lanes*) and 25% of the bound material (*remaining lanes*) were subjected to SDS-PAGE and visualized by staining with Coomassie blue. *Syt*, Cytoplasmic domain of synaptotagmin I. Note: the *asterisk* indicates a proteolytic fragment present in preparations of GST-fused AD3 mutant synaptotagmin. *D,* Data from two oligomerization assays (as described in *C*) were quantified by densitometry, normalized to the pixel intensity in the "total" lanes, and plotted versus the free [Ca^{2+}]. *Closed circles*, Wild-type synaptotagmin; *open circles*, AD3 synaptotagmin. *E,* Soluble *Drosophila* synaptotagmin I (5 μM) was incubated with 30 μg of either wild-type synaptotagmin IV, AD3 synaptotagmin IV, or synaptotagmin IV containing a KK to AA substitution (Chapman et al., 1998) at amino acids 385 and 386. Binding of synaptotagmin I was visualized by Western analysis with anti-synaptotagmin I DSYT2 antisera (Littleton et al., 1993). ● denotes binding reactions lacking soluble synaptotagmin.

took an investigation of the defects resulting from the Y364N change in C2B in the *AD3* mutant to uncover a biochemical link between synaptotagmin, assembly of the SNARE complex, and vesicle fusion.

For this analysis, we engineered the *AD3* mutation into rat synaptotagmin I (corresponding to amino acid 311 in the rat sequence) to be able to use the biochemical reagents available for this organism. One possibility to explain the *AD3* phenotype is that the mutant protein fails to interact with the SNARE complex to trigger Ca^{2+}-induced conformational changes required for fusion. However, both wild-type and *AD3* mutant synaptotagmin showed comparable binding to preassembled SNARE complexes (Fig. 7*C*). Another possibility is that the interaction of synaptotagmin with the synprint domain of the presynaptic Ca^{2+} channel is affected, resulting in an alteration in Ca^{2+} entry that could block the interaction of a second Ca^{2+} sensor with the SNARE components. Although the C2B domain is required for the interaction with synprint, the *AD3* mutation does not affect this interaction (Fig. 7*D*).

The *AD3* mutation lies in close proximity to a set of five conserved amino acid residues that coordinate divalent cations in a number of C2 domains (Fig. 8*A*). These structural data suggest that the *AD3* mutation may impair the putative Ca^{2+}-binding properties of C2B. To test this hypothesis, the C2B domain of wild-type and AD3 mutant rat synaptotagmin were immobilized as GST fusion proteins (the isolated C2B domain of *Drosophila* is insoluble and could not be produced in sufficient quantities to perform this analysis). Fusion proteins were incubated with increasing concentrations of chymotrypsin in the presence of EGTA or Ca^{2+}, and the proteolysis patterns were analyzed by SDS-PAGE. As shown in Figure 8*B*, the degradation patterns in EGTA versus Ca^{2+} were distinct, demonstrating that C2B undergoes a conformational change after binding Ca^{2+}. A protease-resistant fragment accumulated in the presence of Ca^{2+}, suggesting that Ca^{2+} binds to and stabilizes this domain. This result is analogous to the data from limited proteolysis of the C2A domain (Davletov and Sudhof, 1994). In contrast, a different proteolysis pattern was observed with the AD3 mutant C2B domain and the presence of Ca^{2+} has no effect on this pattern. These results suggest that the *AD3* mutation impairs Ca^{2+}-driven conformational changes in C2B. We note that the ability of the AD3 mutant to bind SNARE complexes, AP-2, and the synprint peptide, as described above, demonstrates that the C2B domain is not misfolded, but rather, exhibits a selective loss of function.

The C2B domain of synaptotagmin mediates Ca^{2+}-triggered oligomerization as previously described (Chapman et al., 1996; Sugita et al., 1996; Desai et al., 2000). To determine whether this oligomerization activity is affected by the observed alteration in Ca^{2+}-dependent conformational changes in the AD3 C2B domain, oligomerization of the cytoplasmic domains of wild-type and *AD3 Drosophila* synaptotagmin were assayed at increasing

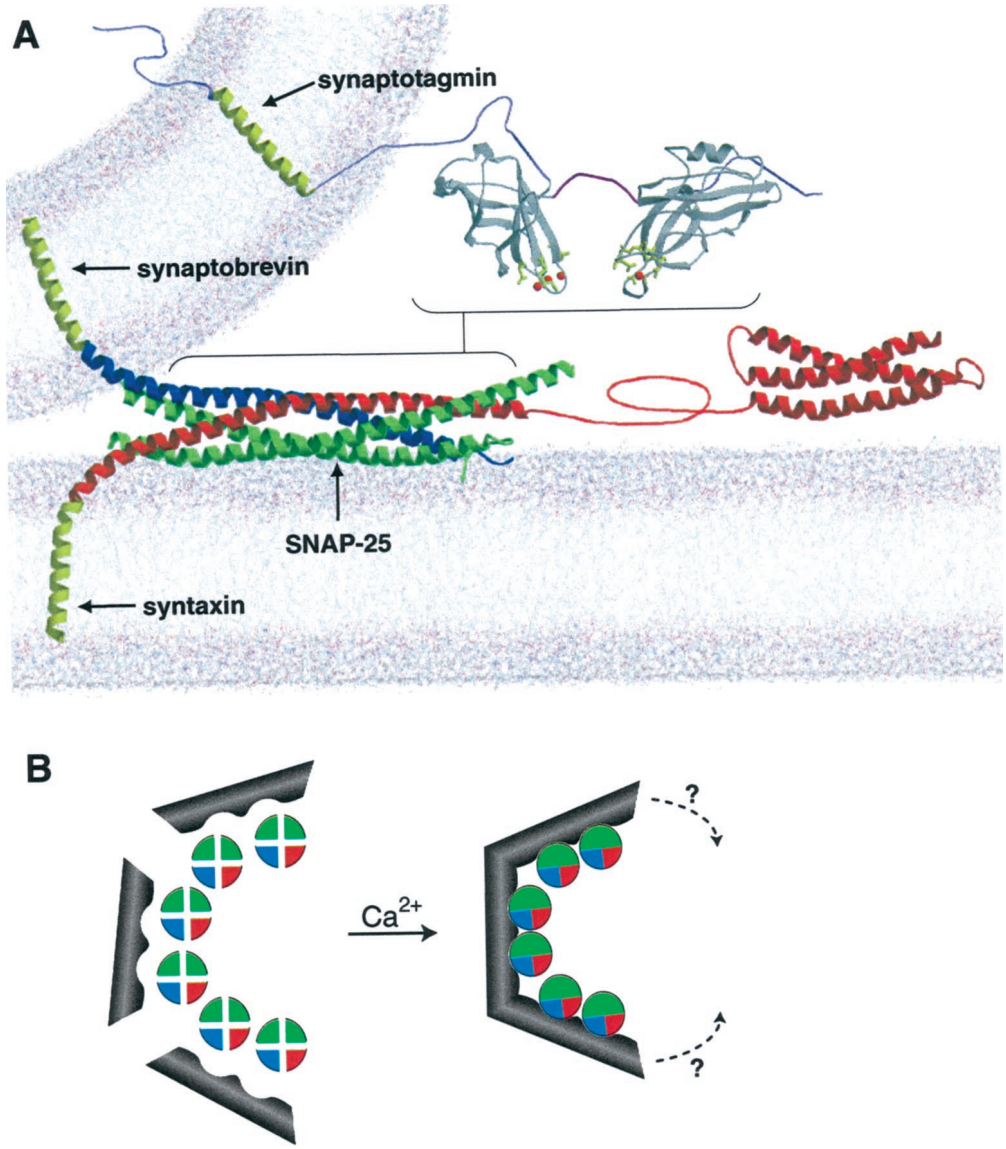

Figure 9. Model depicting the synaptotagmin-SNARE complex. *A,* The core of the SNARE complex, the Habc domain of syntaxin, the cytoplasmic domain of synaptotagmin, and a simulated lipid bilayer were modified from Sutton et al. (1998), Fernandez et al. (1998), Sutton et al. (1999), and Heller et al. (1993), respectively, and rendered using MOLSCRIPT (Kraulis, 1991). The regions that interact are indicated with *brackets*; both C2 domains of synaptotagmin are required for high affinity binding to the base of the SNARE complex (Chapman et al., 1995; Davis et al., 1999; Gerona et al., 2000). The transmembrane anchors of syntaxin, synaptobrevin, and synaptotagmin were generated by molecular modeling. *B,* Model for synaptotagmin-mediated assembly and clustering of SNARE complexes. One synaptotagmin can interact with two SNARE complexes; this interaction is depicted as two grooves within synaptotagmin that bind and assemble SNAREs (which are shown in an "end view" in which each strand of the four-helix bundle is depicted as a quarter of a circle).

concentrations of Ca^{2+}. As shown in Figure 8, *C* and *D*, wild-type synaptotagmin efficiently bound to immobilized synaptotagmin in response to Ca^{2+}. In contrast, Ca^{2+}-triggered oligomerization of the AD3 mutant was reduced to ~40% of the wild-type clustering activity. These data suggest that the *AD3* phenotype results from a defect in the Ca^{2+}-sensing ability of the C2B domain, causing a loss of Ca^{2+}-induced synaptotagmin oligomerization and subsequent SNARE assembly *in vivo*. To obtain additional evidence for this model, we tested whether the AD3 Y to N change also alters Ca^{2+}-dependent oligomerization when introduced into other isoforms of synaptotagmin. As shown in Figure 8*E*, when the AD3 change is engineered into *Drosophila* synaptotagmin IV, Ca^{2+}-dependent hetero-oligomerization with wild-type synaptotagmin I is decreased by >80%. The AD3 mutation disrupted oligomerization as effectively as the well characterized K326,327A substitution within the C2B domain of rat synaptotagmin I (Chapman et al., 1998; Desai et al., 2000; note: this mutation corresponds to K385, K386 in *Drosophila* synaptotagmin IV).

Under our assay conditions, oligomerization of wild-type synaptotagmin was half-maximal at ~6 μM Ca^{2+}. This value is considerably lower than the Ca^{2+} dependence for exocytosis in retinal bipolar neurons (Heidelberger et al., 1994) but is consistent with the Ca^{2+} dependence for exocytosis at the axosomatic synapse formed by the calyx of Held (Bollman et al., 2000; Schneggenburger and Neher, 2000).

DISCUSSION

Mutations in synaptotagmin I result in profound defects in neurotransmitter release. In *Drosophila*, these defects include a severe reduction in evoked release, an increase in spontaneous fusion, and delays in the onset of vesicle fusion (Littleton et al., 1993, 1994; DiAntonio and Schwarz, 1994). In mice, disruption of the synaptotagmin I gene results in the selective loss of the rapid synchronous component of exocytosis without affecting the frequency of spontaneous fusion events (Geppert et al., 1994). In contrast, removal of the t-SNARE syntaxin eliminates both evoked and spontaneous fusion (Schulze et al., 1995), and temperature-sensitive mutations in syntaxin that block SNARE assembly result in paralysis and an accumulation of unfused vesicles at release sites (Littleton et al., 1998). These results are

consistent with mounting functional data indicating that assembly of the SNARE complex is essential for vesicle fusion (Weber et al., 1998; Chen et al., 1999; Xu et al., 1999). The more variable effects on secretion in *synaptotagmin* mutants are consistent with the possibility that synaptotagmin plays a regulatory role in promoting evoked release through direct interactions with the fusion machinery, without being absolutely necessary for vesicle fusion. Here, we provide evidence for two independent functions for the C2B domain of synaptotagmin I in synaptic vesicle cycling. *AD1* mutations, which lack the C2B domain, disrupt synaptotagmin—AP-2 interactions (Zhang et al., 1994) and lead to a fourfold reduction in the total number of synaptic vesicles at mutant terminals during nerve terminal stimulation. These findings are similar to studies of *synaptotagmin* mutants in *C. elegans* (Jorgensen et al., 1995). *AD1* terminals do harbor some synaptic vesicles surrounding active zones and have an elevated frequency of spontaneous fusions when examined electrophysiologically. Thus, it is likely that additional endocytotic pathways are capable of maintaining the smaller pool of vesicles that are recycled in the immediate vicinity of the active zone. Our observations are consistent with the distribution of *Drosophila* AP-2, which is absent near active zones, but concentrated in the synaptic periphery (Gonzalez-Gaitan et al., 1996). The lack of a complete loss of endocytosis in *Drosophila synaptotagmin* null mutants (Reist et al., 1998) also indicates that in unstimulated synapses, other endocytotic pathways that bypass synaptotagmin I can refill nerve terminals given enough time. One possible candidate for mediating this endocytotic trafficking in the absence of synaptotagmin I is synaptotagmin IV, which is also present on synaptotagmin I-containing vesicles and binds to AP-2 as effectively as synaptotagmin I (Li et al., 1995; Littleton et al., 1999).

In contrast with the endocytotic defect manifested in *AD1* mutants, the *AD3* mutant phenotype results from a postdocking defect in synaptic vesicle exocytosis and a failure to assemble SNARE complexes *in vivo*. Our biochemical analysis revealed that this mutation disrupts Ca^{2+}-induced conformational changes in the C2B domain and inhibits Ca^{2+}-induced oligomerization. Whether the failure to assemble SNARE complexes results from a direct defect in the acceleration of SNARE formation by synaptotagmin or an alteration in additional downstream SNARE interactions after synaptotagmin clustering requires further analysis. Nonetheless, these results indicate that the C2B domain of synaptotagmin must be able to bind Ca^{2+}, change conformation, and cluster to trigger coordinated vesicle fusion at nerve terminals. These results provide biochemically supported genetic evidence that synaptotagmin is indeed a Ca^{2+} sensor for fast exocytosis, as proposed in previous studies (Brose et al., 1992; DiAntonio and Schwarz, 1994; Geppert et al., 1994; Littleton et al., 1994). How oligomerization of synaptotagmin leads to vesicle fusion is unknown, but it is likely to involve direct effects on the SNARE complex. We suggest that clustering of SNARE complexes by Ca^{2+}-synaptotagmin leads to rapid triggering of fusion via formation of SNARE-dependent fusion pores. The Ca^{2+}-independent interaction of synaptotagmin with SNAREs would allow these vesicles to remain in a fusion-ready state and may contribute to the suppression of spontaneous fusion events (DiAntonio and Schwartz, 1994, 1999; Littleton et al., 1994). The loss of SNARE clustering activity in synaptotagmin mutants would prevent rapid, Ca^{2+}-dependent vesicle fusion as has been observed in *syt* mutants. The partial rescue of release in *syt* mutants at very high Ca^{2+} levels could reflect the ability of other Ca^{2+} sensors to trigger fusion under these conditions. These other Ca^{2+} sensors might be other members of the synaptotagmin family, which contains seven members in *Drosophila*. Biochemical characterization of the Ca^{2+}-dependent oligomerization properties of these synaptotagmins might uncover other candidates for mediating fusion at high Ca^{2+} concentrations.

Scale models reveal precisely how close complete assembly of the SNARE complex would bring the vesicle and target membranes (Fig. 9*A*; Sutton et al., 1998). A number of experiments indicate that SNARE complexes do not fully assemble before fusion (Chen et al., 1999; Xu et al., 1999). Thus, final "zippering" of the complex may not occur until arrival of the Ca^{2+} signal that triggers fusion (Chen et al., 1999). In this case, Ca^{2+}-triggered oligomerization of synaptotagmin and its association with partially assembled SNARE complexes could drive final assembly of the base of the complex (Chapman et al., 1995; Kee and Scheller, 1996; Davis et al., 1999; Gerona et al., 2000) to accelerate SNARE-mediated membrane fusion and SDS-resistant SNARE complex assembly (Weber et al., 1998). The facilitation of SNARE complex assembly, *in vitro* and *in vivo*, reported here supports this model. Furthermore, Ca^{2+}-synaptotagmin triggers the formation of disulfide-bonded SNARE complex dimers. This finding, in conjunction with the 1:2 stoichiometry of saturated synaptotagmin-SNARE complexes, argues that Ca^{2+}-synaptotagmin can bring at least two SNARE complexes into close proximity. The ability of synaptotagmin to oligomerize and simultaneously bind SNAREs suggests that synaptotagmin can cluster multiple SNARE complexes into a higher ordered assembly that might correspond to the exocytotic fusion pore. In this light we point out that SNARE complexes alone appear to cluster only weakly (Fasshauer et al., 1997; Hohl et al., 1998; but see also Poirier et al., 1998) and that viral fusion proteins are homotrimers that must assemble into oligomers to form functional fusion pores (Blumenthal et al., 1996; Danieli et al., 1996). Similarly, a protein designated EEA1 has recently been reported to cluster syntaxin-13 into oligomeric structures that are required for endosomal fusion (McBride et al., 1999). An analogous model for synaptotagmin in neuronal exocytosis is shown in Figure 9. Synaptotagmin binds to the membrane proximal region of the SNARE complex while simultaneously penetrating into membranes (Davis et al., 1999; Gerona et al., 2000; Fig. 9*A*). We speculate that these interactions, in conjunction with the ability of synaptotagmin to oligomerize and to facilitate SNARE complex assembly (Fig. 9*B*), leads to formation of an open fusion pore. In support of this model, we have recently shown that disrupting C2B-mediated oligomerization of synaptotagmin I *in vitro* can lead to postdocking vesicle fusion defects in cracked PC12 cells (Desai et al., 2000).

Finally, we point out that the N terminus of synaptotagmin contains a novel Ca^{2+}-independent clustering domain that may play an important role in both endocytosis (von Poser et al., 2000) and exocytosis (Bai et al., 2000). We speculate that N-terminal clustering activity, in conjunction with the weak Ca^{2+}-independent components of C2B-C2B and synaptotagmin–SNARE interactions, may serve to poise synaptotagmin–SNARE complexes for rapid conformational changes, including the formation of a stable ring-like structure, in response to a rise in intracellular Ca^{2+}.

In summary, our data indicate that the C2B domain of synaptotagmin must "sense" Ca^{2+} and assemble into clusters, for docked synaptic vesicles to undergo synchronous exocytosis.

These data further suggest Ca^{2+}–synaptotagmin can regulate SNARE complex dynamics, thus providing a compelling connection between the Ca^{2+} sensor for exocytosis and the SNARE fusion machinery.

REFERENCES

Bai J, Earles C, Lewis J, Chapman ER (2000) Membrane-embedded synaptotagmin interacts with cis and trans target membranes and assembles into oligomers via a novel mechanism. J Biol Chem 275:25427–25435.

Bark IC, Wilson MC (1994) Human cDNA clones encoding two different isoforms of the nerve terminal protein SNAP-25. Gene 139:291–292.

Bennett MK, Calakos N, Scheller RH (1992) Syntaxin: a synaptic protein implicated in docking of synaptic vesicles at presynaptic active zones. Science 257:255–259.

Blumenthal R, Sarkar DP, Durell S, Howard DE, Morris SJ (1996) Dilation of the influenza hemagglutinin fusion pore revealed by kinetics of individual cell-cell fusion events. J Cell Biol 135:63–71.

Bollman JH, Sakmann B, Borst JGG (2000) Calcium sensitivity of glutamate release in a Calyx-type terminal. Science 289:953–957.

Brose N, Petrenko AG, Sudhof TC, Jahn R (1992) Synaptotagmin: a Ca^{2+} sensor on the synaptic vesicle surface. Science 256:1021–1025.

Chapman ER, Jahn R (1994) Calcium-dependent interaction of the cytoplasmic region of synaptotagmin with membranes. J Cell Biol 269:5735–5741.

Chapman ER, Hanson PI, An S, Jahn R (1995) Ca^{2+} regulates the interaction between synaptotagmin and syntaxin 1. J Biol Chem 270:23667–23671.

Chapman ER, An S, Edwardson JM, Jahn R (1996) A novel function for the second C2 domain of synaptotagmin: Ca^{2+}-triggered dimerization. J Biol Chem 271:5844–5849.

Chapman E, Desai R, Davis A, Tornehl C (1998) Delineation of the oligomerization, AP-2 binding, and synprint binding region of the C2B domain of synaptotagmin. J Biol Chem 273:32966–32973.

Chen YA, Scales SJ, Patel SM, Doung YC, Scheller RH (1999) SNARE complex formation is triggered by Ca^{2+} and drives membrane fusion. Cell 97:165–174.

Danieli T, Pelletier SL, Henis YI, White JM (1996) Membrane fusion mediated by the influenza virus hemagglutinin requires the concerted action of at least three hemagglutinin trimers. J Cell Biol 133:559–569.

Davis AF, Bai J, Fasshauer D, Wolowick MJ, Lewis JL, Chapman ER (1999) Kinetics of synaptotagmin responses to Ca^{2+} and assembly with the core SNARE complex onto membranes. Neuron 24:363–376.

Davletov BA, Südhof TC (1994) Ca^{2+}-dependent conformational change in synaptotagmin I. J Biol Chem 269:28547–50.

Desai R, Vyas B, Earles C, Littleton JT, Kowalchyck J, Martin TFJ, Chapman ER (2000) The C2B-domain of synaptotagmin is a Ca^{2+} sensing module essential for exocytosis. J Cell Biol 150:1125–1135.

DiAntonio A, Schwarz TL (1994) The effect on synaptic physiology of synaptotagmin mutations in *Drosophila*. Neuron 12:909–920.

Elferink LA, Trimble WS, Scheller RH (1989) Two vesicle-associated membrane protein genes are differentially expressed in the rat central nervous system. J Biol Chem 264:11061–11064.

Fasshauer D, Otto H, Eliason WK, Jahn R, Brünger AT (1997) Structural changes are associated with soluble *N*-ethylmaleimide-sensitive fusion protein attachment receptor complex formation. J Biol Chem 272:28036–28041.

Fasshauer D, Eliason WK, Brunger AT, Jahn R (1998) Identification of a minimal core of the synaptic SNARE complex sufficient for reversible assembly and disassembly. Biochemistry 37:10345–10353.

Fasshauer D, Antonin W, Margatti M, Pabst S, Jahn R (1999) Mixed and non-cognate SNARE complexes. J Biol Chem 274:15440–15446.

Fernandez I, Ubach J, Dulubova I, Zhang X, Südhof TC, Rizo J (1998) Three-dimensional structure of an evolutionarily conserved N-terminal domain of syntaxin 1A. Cell 94:841–849.

Fiebig KM, Rice LM, Pollock E, Brunger AT (1999) Folding intermediates of SNARE complex assembly. Nat Struct Biol 6:117–123.

Geppert M, Goda Y, Hammer RE, Li C, Roshal TW, Stevens CF, Sudhof TC (1994) Synaptotagmin I: a major Ca^{2+} sensor for transmitter release at a central synapse. Cell 79:717–727.

Gerona RRL, Larsen EC, Kowalchyk JA, Martin TFJ (2000) The C terminus of SNAP25 is essential for Ca^{2+}-dependent binding of synaptotagmin to SNARE complexes. J Biol Chem 275:6328–6336.

Gonzalez-Gaitan M, Jackle H (1996) Role of *Drosophila* α-adaptin in presynaptic vesicle recycling. Cell 88:767–776.

Hanson PI, Heuser JE, Jahn R (1997) Neurotransmitter release-four years of SNARE complexes. Curr Opin Neurobiol 7:310–315.

Hayashi T, McMahon H, Yamasaki S, Binz T, Hata Y, Sudhof TC, Niemann H (1994) Synaptic vesicle membrane fusion complex: action of clostridial neurotoxins on assembly. EMBO J 13:5051–5061.

Heidelberger R, Heinemann C, Matthews G (1994) Ca^{2+} dependence of the rate of exocytosis in a synaptic terminal. Nature 371:513–515.

Heller H, Schaefer K, Schulten K (1993) Molecular dynamics simulation of a lipid bilayer of 200 lipids in the gel and liquid crystal phases. J Phys Chem 97:8343–8360.

Hohl TM, Parlati F, Wimmer C, Rothman JE, Söllner TH, Engelhardt H (1998) Arrangement of subunits in 20 S particles consisting of NSF, SNAPs, and SNARE complexes. Mol Cell 2:539–548.

Jahn R, Südhof TC (1999) Membrane fusion and exocytosis. Annu Rev Biochem 68:863–911.

Jorgensen EM, Hartwieg E, Schuske K, Nonet ML, Jin Y, Horvitz HR (1995) Defective recycling of synaptic vesicles in synaptotagmin mutants of *Caenorhabditis elegans*. Nature 378:196–199.

Katz B (1969) The release of neural transmitter substances. Liverpool: Liverpool UP.

Kee Y, Scheller RH (1996) Synaptotagmin-binding domains of syntaxin. J Neurosci 16:1975–1981.

Kraulis PJ (1991) MOLSCRIPT: a program to produce both detailed and schematic plots of protein structures. J Appl Crystal 24:946–950.

Li C, Ullrich B, Zhang JZ, Anderson RGW, Brose N, Südhof TC (1995) Ca^{2+}-dependent and independent activities of neural and non-neural synaptotagmins. Nature 375:594–599.

Littleton JT, Stern M, Schulze K, Perin M, Bellen HJ (1993) Mutational analysis of *Drosophila* synaptotagmin demonstrates its essential role in Ca^{2+}-activated neurotransmitter release. Cell 74:1125–1134.

Littleton JT, Stern M, Perin M, Bellen HJ (1994) Calcium dependence of neurotransmitter release and rate of spontaneous vesicle fusions are altered in *Drosophila* synaptotagmin mutants. Proc Natl Acad Sci USA 91:10888–10892.

Littleton JT, Chapman ER, Kreber R, Garment MB, Carlson SD, Ganetzky B (1998) Temperature-sensitive paralytic mutations demonstrate that synaptic exocytosis requires SNARE complex assembly and disassembly. Neuron 21:401–413.

Littleton JT, Serano TL, Rubin GM, Ganetzky B, Chapman ER (1999) Synaptic function modulated by changes in the ratio of synaptotagmin I and IV. Nature 400:757–760.

Llinas R, Steinberg IZ, Walton K (1981) Presynaptic Ca^{2+} currents in squid giant synapse. Biophys J 33:289–322.

Matthew WD, Tsavaler L, Reichardt LF (1981) Identification of a synaptic vesicle-specific protein with a wide tissue distribution in neuronal and neurosecretory tissue. J Cell Biol 91:257–269.

McBride HM, Rybin V, Murphy C, Giner A, Teasdale R, Zerial M (1999) Oligomeric complexes link rab5 effectors with NSF and drive membrane fusion via interactions between EEA1 and syntaxin 13. Cell 98:377–386.

Nonet ML, Grundahl K, Meyer BJ, Rand JB (1993) Synaptic function is impaired but not eliminated in *C. elegans* mutants lacking synaptotagmin. Cell 7:1291–1305.

Osborne SL, Herreros J, Bastiaens PI, Schiavo G (1999) Calcium-dependent oligomerization of synaptotagmins I and II. J Biol Chem 274:59–66.

Oyler GA, Higgins GA, Hart RA, Battenberg E, Billingley M, Bloom FE, Wilson MC (1989) J Cell Biol 109:3039–3052.

Perin MS, Fried VA, Mignery GA, Jahn R, Südhof TC (1990) Phospholipid binding by a synaptic vesicle protein homologous to the regulatory region of protein kinase C. Nature 345:260–263.

Poirier MA, Hao JC, Malkus PN, Chan C, Moore MF, King DS, Bennett MK (1998a) Protease resistance of syntaxin/SNAP-25/VAMP complexes. Implications for assembly and structure. J Biol Chem 273:11370–11377.

Poirier MA, Xiao W, Macosko JC, Chan C, Shin YK, Bennett MK (1998b) The synaptic SNARE complex is a parallel four-stranded helical bundle. Nat Struct Biol 5:765–769.

Reist NE, Buchanan J, Li J, DiAntonio A, Buxton EM, Schwarz TL (1998) Morphologically docked synaptic vesicles are reduced in synaptotagmin mutants of *Drosophila*. J Neurosci 18:7662–7673.

Rothman JE (1994) Mechanisms of intracellular membrane transport. Nature 372:55–63.

Scheller RH (1995) Membrane trafficking in the presynaptic nerve terminal. Neuron 14:893–897.

Schiavo G, Stenbeck G, Rothman JE, Söllner TH (1997) Binding of the synaptic vesicle v-SNARE, synaptotagmin, to the plasma membrane t-SNARE, SNAP-25, can explain docked vesicles at neurotoxin-treated synapses. Proc Natl Acad Sci USA 94:997–1001.

Schneggenburger R, Neher E (2000) Intracellular calcium dependence of transmitter release rate of a fast central synapse. Nature 406:889–893.

Schulze K, Broadie K, Perin M, Bellen HJ (1995) Genetic and electrophysiological studies of *Drosophila* syntaxin-1A demonstrate its role in nonneuronal secretion and neurotransmission. Cell 80: 311–320.

Sheng ZH, Yokoyama CT, Catterall WA (1997) Interaction of the synprint site of N-type Ca^{2+}-channels with the C2B domain of synaptotagmin I. Proc Natl Acad Sci USA 94:5405–5410.

Söllner T, Whiteheart SW, Brunner M, Erdjument-Bromage H, Geromanos S, Tempst P, Rothman JE (1993) SNAP receptors implicated in vesicle targeting and fusion. Nature 362:318–324.

Südhof TC, Rizo J (1996) Synaptotagmins: C2-domain proteins that regulate membrane traffic. Neuron 17:379–388.

Sugita S, Hata Y, Südhof TC (1996) Distinct Ca^{2+}-dependent properties of the first and second C2-domains of synaptotagmin. J Biol Chem 271:1262–1265.

Sutton RB, Fasshauer D, Jahn R, Brunger AT (1998) Crystal structure of a SNARE complex involved in synaptic exocytosis at 2.4 A resolution. Nature 395:347–353.

Sutton RB, Ernst JA, Brunger AT (1999) Crystal structure of the cytosolic C2A-C2B domains of synaptotagmin III: implications for Ca^{2+}-independent SNARE complex formation. J Cell Biol 147:589–598.

Trimble WS, Cowan DM, Scheller RH (1988) VAMP I: a synaptic vesicle-associated integral membrane protein. Proc Natl Acad Sci USA 85:4538–4542.

von Poser C, Zhang JZ, Mineo C, Ding W, Ying YS, Sudhof TC, Anderson RGW (2000) Synaptotagmin regulation of coated pit assembly. J Biol Chem 275:30916–30924.

Weber T, Zemelman BV, McNew JA, Westermann B, Gmachl M, Parlati F, Sollner TH, Rothman JE (1998) SNAREpins: minimal machinery for membrane fusion. Cell 92:759–772.

Xu T, Rammer B, Margittai M, Artalejo AR, Neher E, Jahn R (1999) Inhibition of SNARE complex assembly differentially affects kinetic components of exocytosis. Cell 99:713–722.

Zhang JZ, Davletov BA, Sudhof TC, Anderson RG (1994) Synaptotagmin I is a high affinity receptor for clathrin AP-2: implications for membrane recycling. Cell 78:751–760.